33RD CONGRESS
OF THE INTERNATIONAL COUNCIL
OF THE AERONAUTICAL SCIENCES
STOCKHOLM, SWEDEN, 4-9 SEPTEMBER, 2022

ICAS 2022 SWEDEN

PERFORMANCE BENEFITS OF A FAN ON BLADE – FLADE – FOR A VARIABLE CYCLE ENGINE

Marcelo Assato[1], Ali Altar Inceer[2], Lucilene Moraes[3], JesuinoTakachi Tomita[3], Cleverson Bringhenti[3], Pedro Bravo-Mosquera[4], Daniel Rosell[5], Tomas Grönstedt[2, *]

[1]Institute of Aeronautics and Space (IAE), Propulsion Division, São José dos Campos, SP, Brazil
[2]Chalmers University of Technology, Fluid Dynamics, Mechanics and Maritime Sc., Göteborg, Sweden
[3]Aeronautics Institute of Technology (ITA), Turbomachines Department, São José dos Campos, SP, Brazil
[4]Department of Aeronautical Engineering, University of São Paulo, São Carlos, Brazil
[5]SAAB Aeronautics, Bröderna Ugglas Gata, 581 88 Linköping, Sweden

*Correspondingauthor

Email addresses: Marcelo Assato: marceloma@fab.mil.br, Tomas Grönstedt: tomas.gronstedt@chalmers.se

Abstract

Variable cycle engines promise to enable adaptive cycles that give close to optimal performance over a wide range of conflicting mission requirements, such as low altitude high speed flight and supercruise still providing excellent range. Modelling such engines pose challenges for general purpose software since variable geometry gas paths modify the underlying set of equations being solved. It is possible to use multiple engine models transferring design data between the models. This, however, creates a high risk for inconsistency and modelling error. It is more attractive if the solutions obtained could be determined using the same model. In this work an in-house software was developed to model an Adaptive Cycle Engine (ACE). This development was used to show how variable cycle mode switches can be integrated into general purpose performance tools. The variable cycle engine uses a FLADE, which is a "fan on blade" component, to extend its range and to provide improved subsonic performance. The individual impact of the components, its effect on propulsion performance parameters and in the engine installation were analyzed as the main results. The contribution from this paper is thus two-fold, firstly the paper goes ahead and proposes new methods for the simulation of mode switching in generic performance tools by introducing dynamic equation systems. Secondly, the paper then studies the FLADE component and its potential performance benefits if added to a conventional turbofan architecture.

Keywords: Variable cycle engine (VCE), FLADE (Fan on bLADE), Turbofan, Adaptive Cycle Engine (ACE), VCE mode switch

1. Introduction

The demand for advanced propulsion systems for future fighters has increased over the recent decades. This is to a large degree driven by a need to meet the conflicting requirements of high specific thrust for high flight velocities and low specific thrust conditions for efficient cruise efficiency combined with high absolute thrust levels for short take-off low altitude combat maneuvering [1, 2]. To fulfill these seemingly conflicting criteria Variable Cycle Engines (VCE) have been proposed as potential candidates. Such systems have the capability to use variable geometry features within the engine, changing the bypass ratio and fan pressure ratio in flight. This allows the engine to better match its conflicting criteria potentially outperforming conventional turbofan designs.

Research into VCEs has been ongoing since the 1950's, initiated by the United States Supersonic Commercial Air Transport program. This work led to highlighting the need for an engine that could be optimized for both supersonic and subsonic flights [3]. In the 1980's GE Aircraft Engines (GEAE) identified a promising system, the double-bypass VCE concept. The cycle selection, configuration, evaluation, building and flight testing was then carried out through the Advanced Tactical Fighter (ATF) program. The engine demonstrated high specific thrust and good efficiency at part-power; it combined the performance of a moderate bypass ratio turbofan at subsonic flight conditions with the performance of a turbojet in supersonic flight [3]. The development contributed greatly to increasing the confidence and total understanding of the double-bypass VCE. In September 1990 the VCE alternative for the ATF reached a supercruise, Mach number of 1.58 during a test flight, whereas its competitor configuration only reached Mach 1.43 [4]. Although, eventually not selected for the F-22 Raptor, the VCE architecture showed great promise for future emerging programs.

More recently, the US announced its VCE program Adaptive Versatile Engine Technology (ADVENT) targeting a 25% average fuel burn reduction using technologies such as cooled cooling [5, 6]. In 2012, GE was chosen to continue its ADVENT program into the Adaptive Engine Technology Development (AETD) program under the US Air Force Research Laboratory [6, 7]. Over the last years important progresses have been made for the adaptive cycle engines. In 2019, GE Aviation announced that has completed the detailed design of its XA100 engine to meet the AETP program requirements where the new engine ramps up thrust by 10 percent while simultaneously improving fuel efficiency by 25% compared to a typical fighter jet engine [8].

As part of the GE work in the ADVENT program a third-stream was added to the engine acting as cooling heat sink [8]. This technology, that is adding a second bypass stream, has attracted attention by several researchers suggesting that it provides significant benefits. Lately, many studies have analyzed a new type of VCE, the Adaptive Cycle Engine (ACE) having a third duct circumscribing a variable cycle inner gas turbine engine. According to [1, 9] this “third stream” brings a number of possibilities, such as providing a cool heat sink for dissipating aircraft heat loads, cooling turbine cooling air, as well as that airflow can independently be modulated so that engine airflow demand can be matched with the available inlet flow at a variety of operating points. This allows reducing spillage drag and increases propulsive efficiency.

The current paper develops a model for the ACE cycle as well as relating it to a conventional turbofan engine by using a previously published reference cycle [10]. Although the performance modelling of variable cycle engines can be done by the solution of a small system of non-linear equations, an uncareful setup of the model will create a singular equation system. A remedy for such efforts is to develop different sets of equations for the different modes [11, 12]. This is equivalent to having separate engine models with interrelated design parameters. As an alternative, only one system model may be used, typically the most general form where all flow paths open. Closing of gas paths may then be numerically modelled by very small flows through the use of variable geometry parameters representing closing nozzles, variable turbine areas, variable valves and similar [9]. This work develops an alternative strategy for solving the equation system, where the set of equations in use may change dynamically through the simulation. Closing a bypass duct then means that the iteration variable relevant for the particular duct will be sorted out of the active equation system by algorithmic logic. This must also include corresponding residuals for this flow path, still maintaining thermodynamic design areas for other active components in the engine.

The double bypass variable cycle engine [3] and the adaptive cycle engine [13] are the most frequently proposed variable cycle engines in the aero engine literature, promising to supplant the conventional turbofan cycle. Actually, the two cycles, as well as the turbofan, are closely related. If the FLADE or fan on blade component is shut down by completely closing its exhaust nozzle the ACE cycle transforms into a double bypass cycle. In turn, if the bypass injector located downstream of the core driven fan stage of the double bypass engine is closed, a conventional turbofan architecture is obtained. Until now, existing literature has only studied the FLADE component integrated on a double bypass cycle. However, it is quite feasible to add the FLADE component directly to a turbofan architecture without introducing the features of the double bypass engine. This will give the engine a more limited range of variable cycle engine features, but it will also reduce the complexity of the engine. It is interesting to study, in isolation, how the addition of a FLADE component influences the performance of a turbofan, and that is a key topic for this work.

The contribution from this paper is thus two-fold, firstly the paper goes ahead and develops new methods for the simulation of mode switching in generic performance tools by introducing dynamic equation systems. Secondly, the paper then studies the FLADE component and its potential performance benefits if added to a conventional turbofan architecture.

2. Variable cycle engine modelling and the reference turbofan

The key propulsion system performance data are show in Table 1. Further detail is found in [10].

Table 1: Design point characteristic [10]

Parameter	Design point
Altitude [m]	0 m
Mach number	0
Fan pressure ratio	5.4
HPC pressure ratio	5.8
Inlet mass flow	90 kg/s
Turbine inlet temperature at ISA	1950 K

The data given in Table 1 above is then used to derive the initial cycle also for the ACE concept. The basic architecture is displayed in Figure 1 below.

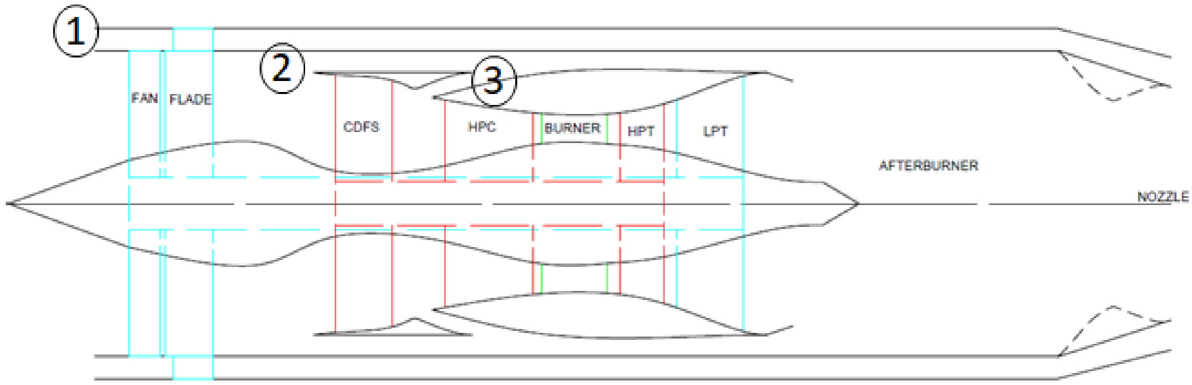

Figure 1: Schematic sketch for ACE engine architecture

To establish a starting point for comparison between the cycles, key parameters for the ACE engine can be derived from the data given in Table 1. The HPC pressure ratio needs to be split into the core drive fan stage and the additional stages in the HPC. The FAN and FLADE components need to be designed to deliver consistent pressure ratios. The feasible pressure ratio on the FLADE will be related to which fan stage it is connected. Note that the FLADE, in its basic form, will only comprise a single stage fan whereas the core flow path of the fan will typically be a multistage design. To compare the performance between a turbofan and a fladed turbofan the inlet mass flow is assumed to remain the same for the two cycles.

2.1 VCE and mode switches in generic software

Modelling variable cycle engines can be done by programming specific code sections for the different modes of the engine, maintaining consistency between the modes by a careful use of design data [11, 12]. Alternatively, the most general mode, that is the mode where all flow paths are open, is used to simulate all other modes as well. This is achieved by designing the engine in the "all open" mode and then simulating other modes by setting relevant valves and injectors to "almost" closed. For the ACE cycle the "all open" mode would correspond to that all three bypass ducts are open and that other modes of operation would involve setting variable bypass injectors (VABIs) and nozzle areas to very small flows thus approximating the closed setting. This creates numerical challenges such as having to handle small negative flows during iteration, and it may also create ill conditioned models and low numerical accuracy. Another drawback is that the design point always needs to be set in the "all open" condition. Frequently, studies for maximum specific thrust such as peak performance during supercruise are more conveniently studied if closed modes can be used for the design point. This then allows supercruise conditions to be set exactly and other conditions may then be handled as off-design points.

For the reasons stated above a somewhat different approach has been devised to handle the engine mode switches. It should be emphasized that the process described here merely discusses some possible remedies to numerical challenges associated with simulating variable cycle engines. For the ACE cycle the following five variable cycle modes are identified:

1. **All open** mode: all three bypass ducts are active.
2. **Double bypass** mode: all flow entering the inlet will be ducted in the inner part of the fan, closing down the FLADE nozzle, that is BPR1=0.0. This mode is referred to as double bypass mode because the active part of the engine actually constitutes a double bypass engine.
3. **High-speed turbofan** mode: This configuration instead shuts down the second bypass option such that BPR2=0.0 and BPR1=0.0. The core driven fan stage could thermodynamically now be seen as additional compression stage of the fan adding to the fan pressure ratio making the cycle ideal for high-speed operation.
4. **Turbofan** mode: The third duct is now also closed down, that is BPR3=0.0 and BPR1=0.0. With all flow leaving the core driven fan stage now entering the core of the engine the cycle is effectively a turbofan cycle.
5. **Range extending turbofan** mode: This configuration instead shuts down the third bypass such that BPR3=0.0 but maintains the FLADE active.

In addition, an additional variable cycle mode may be defined. If the first bypass is open, thus actively using the FLADE, it is possible to set BPR2=0.0. Clearly, this does not make much sense since this would combine a mode where a low specific thrust is targeted with a mode that attempts to establish a high specific thrust. Hence, this configuration is expected to be non-optimal under all relevant conditions and is not studied further in this work.

Table 2: Conventional turbofan equation system and ACE equation system

Turbofan Iteration Variables	ACE iteration Variables	Turbofan Residuals	Turbofan Residuals
Inlet mass flow	Inlet mass flow	Inlet flow compatibility	Inlet flow compatibility
Fan map β	Fan map β	Core flow compatibility	Core flow compatibility
Fan rotation speed	Fan rotational speed	Fan/LPT work compatibility	Fan/LPT work compatibility
Bypass ratio	Bypass ratio (2)	HPC/HPT work compatibility	HPC/HPT work compatibility
HPC map β	HPC map β	HPT inlet flow compatibility	HPT inlet flow compatibility
HPC rotation speed	HPC rotation speed	LPT inlet flow compatibility	LPT inlet flow compatibility
Fuel schedule βf	Fuel schedule βf	Static pressure match in unifier	Static pressure match in unifier
HPT outlet pressure	HPT outlet pressure	Afterburner flow compatibility	Afterburner flow compatibility
LPT outlet pressure	LPT outlet pressure	Engine control residual	Engine control residual
	Bypass ratio upstream of splitter (1)		FLADE nozzle flow compatibility
	FLADE map β		Core driven fan stage / HPC mass flow compatibility
	Bypass ratio downstream of core driven fan stage (3)		Static pressure match in core driven fan stage unifier
	Core driven fan stage map β		FLADE/splitter mass flow compatibility

To understand how the equation system for the variable cycle engine is established it is instructive to compare the model system of equations for the “all open mode” of the ACE architecture with a turbofan engine cycle, as shown in Table 2.

For this work an in-house developed software called GESTPAN [14] is used. Iteration variables are kept track of by separating the iteration values and the structures keeping track of which module input that is iterated in. GESTPAN allows any number of inputs to be connected together. As an example, the FLADE, the FAN and the LPT rotational speed all need to be the same and iterated in. Hence even though the equation solver updates only one variable the algorithm copies the updates to all inputs. To enable closing down the FLADE a new routine, delete_iteration_variable(), was programmed allowing to shut down any iteration variable based on its name and module belonging. In a generic code, with the solution described above, it is then necessary to check whether the iteration variable is used in multiple modules and to remove it from the connection structures used in the program. By addressing the pointer structure like this, the routines normally used to build the system Jacobian and the iteration process can be re-run without change. A corresponding delete_residual() routine was also formed.

The method is demonstrated by designing the engine in all open mode and then switching to double bypass mode. The delete_iteration_variable is used to remove the FLADE beta variable from the iteration system and simultaneously cancelling out the mass flow compatibility equation for the nozzle. It was decided not to develop delete_module() routines but to instead cancel the influence of the third bypass on the engine performance. This was done by embedding (stepwise iteratively solve) the FLADE mass flow the third bypass nozzle thrust and the FLADE torque using multiplier factors for all three parameters going from 1.0 to 0.0 during the iteration process.

2.1 The FLADE performance impact

To illustrate the impact of the FLADE component some basic off-design studies are now presented. Firstly, the conventional turbofan mode (BPR1=0.0 and BPR3=0.0) is presented in Table 3. The design point and off-design point conditions are calculated for sea level static and for M=0.90 alt=9144 m respectively. The major change from the design point to the off-design cruise point are the ambient conditions and a reduced thrust requirement. The cruise point is chosen for a later comparison of an optimized cycle intended to be characteristic for a long-range mission. As seen from the data, the BPR increases at off-design which is characteristic for reducing turbofan thrust. The OPR is reduced indicating a lower rating in the cruise point. Comparing with the cycle data set by the authors in [10], the altitude thrust has been modified somewhat due to an update in aircraft model.

Table 3: Performance data for the conventional turbofan mode (BPR1=0.0 and BPR3=0.0).

ALT	M_0	P_2	T_2	W_2	P_{T3}	T_3	P_{T4}	T_4	P_{T5}	T_5	ABmod
[m]	[-]	[kPa]	[K]	[kg/s]	[kPa]	[K]	[kPa]	[K]	[kPa]	[K]	[-]
0.0	0.0	90.2	288.2	90	2706	814	2598	1950	487	1260	unlit
9144.0	0.9	50.3	265.9	33.9	798	636	764	1472	152	944	unlit

ALT	M_0	BPR2	OPR	F_N	η_{th}	η_p	SFC	vcore
[m]	[-]	[-]	[kPa]	[kN]	[-]	[-]	[mg/N*s]	[m/s]
0.0	0.0	0.45	30	72.0	0.433	0.000	22.66	865
9144.0	0.9	0.58	15.9	16.15	0.458	0.540	25.40	741

To understand the impact of the FLADE on the engine performance it is illustrative to compare the range extending turbofan mode (mode 4) with the pure turbofan mode (mode 4) as presented in Table 4.

Comparing the two modes it is possible to see that the use of the FLADE actually decreases the propulsive efficiency slightly to 0.538 from 0.537. This is despite that the propulsive efficiency from the FLADE stream only, as based on the exhaust velocity, is close to 93%. As discussed below, this happens due to the small proportion of propulsive energy contained in the FLADE jet stream. The SFC is also higher for the FLADE configuration.

Table 4: Range extending turbofan mode (BPR1=0.1, BPR3=0.0), and mode switch to turbofan mode reducing BPR1 to 0.0. Design at SLS.

Mode	ALT	M_0	P_2	T_2	W_2	P_{T3}	T_3	P_{T4}	T_4	P_{T5}	T_5	ABmod
[-]	[m]	[-]	[kPa]	[K]	[kg/s]	[kPa]	[K]	[kPa]	[K]	[kPa]	[K]	[-]
5	0.0	0.0	90.2	288.2	90	2,706	813.6	2598	1950	472	1252	unlit

5	9144.0	0.9	50.18	265.87	35.92	857.4	649.17	820.7	1501.6	156.3	955.2	unlit
4	9144.0	0.9	50.33	265.87	32.24	832.7	643.86	797.2	1496.8	157.0	957.9	unlit

Mode	ALT	M_0	BPR1	BPR2	OPR	F_N	η_{th}	η_p	SFC	vcore	vflade
[-]	[m]	[-]	[-]	[-]	[-]	[kN]	[-]	[-]	[mg/N*s]	[m/s]	[m/s]
5	0.0	0.0	0.1	0.450	30.01	74.0	0.439	0.000	22.08	856.4	314.3
5	9144.0	0.9	0.1	0.564	17.09	16.15	0.467	0.537	25.19	754.6	311.6
4	9144.0	0.9	0.0	0.601	16.55	16.15	0.479	0.538	24.49	754.3	0.0

Taking a closer look at the excess kinetic energies of the two jet streams the relative proportion of energy from the FLADE stream is only 0.06% of the total. This is despite the fact that the mass flow through the FLADE is close to 10% of the total. This obviously derives from the fact that the FLADE jet velocity it is only 14% higher than the flight speed (273 m/s). Hence, it stems from the small net thrust from this stream. This also means that under these conditions the FLADE stream primarily generates additional irreversibility for the engine and contributes to decreasing the efficiency of the engine. Notice that the same installation losses are accounted for the FLADE stream as the stream going into the core.

It is argued that the main benefits that can be developed from the FLADE system, with respect to range, have to originate from the following factors:

1. A lowering of the flight speed to proportionally increase the fraction of thrust generated from the FLADE stream
2. Providing an installation space that can be used for heat rejection, for instance integrating a heat exchanger that rejects heat from cooling the cooling air.
3. Inlet matching, that is recovering spillage drag [9].

If the three factors above are used to establish a performance benefit, any additional weight and installation effect of the FLADE needs to be included in the analysis. In this study we continue to elaborate on how to install the FLADE in the engine system and explore the potential benefit of the FLADE system by a reduction of flight speed (Factor 1 above).

2.2 Description of the FLADE component and characteristics

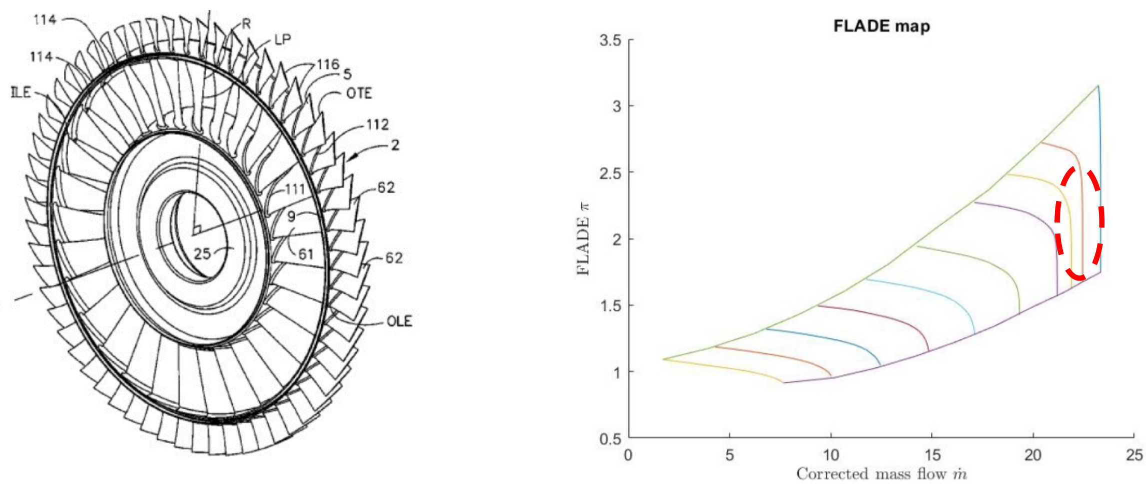

Figure 2: Left: FLADE geometry showing the outer and inner sections of the geometry [15]. Right: A FLADE map obtained by scaling.

As seen in the left of Figure 2 above the FLADE component is mechanically fixed to the inner part constituting one of the fan rotor blade rows. This means that the FLADE portion will run at a very high blade speed and be operating with a high relative Mach number. Hence a careful design is needed to not compromise turbomachinery efficiency. It is also likely that the FLADE flow variability close to the design speed is quite limited in corrected flow showing a characteristic behavior similar to what is indicated by the read ellipse in the map above. The major mass flow variation through the

FLADE system must thus be achieved by varying the pressure ratio over the FLADE. This is done most simply by a variable exhaust nozzle for the FLADE stream. Very crudely, visually estimating directly from the FLADE map a ±25% variation from the nominal condition may be achieved. With a BPR of say 0.2 this would amount to a ±10% variation in engine mass flow assuming that the core may run unaffected. Hence the ability to achieve a variable mass flow matching intake spillage should be substantial.

Another effect that influences the design of the FLADE operability is the FLADE FPR. Clearly, it is difficult to increase the design pressure ratio much beyond 2.0 for a single stage fan. Of course, multiply FLADED stages could be considered but this would increase complexity substantially. Looking at how off-design points move with FLADE FPR we see that cruise variability is limited by increasing the FLADE FPR.

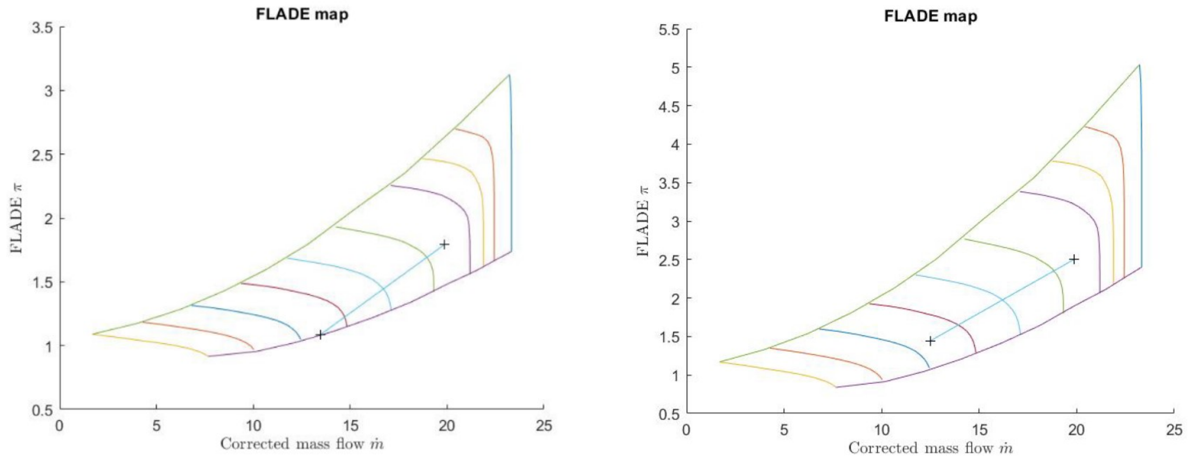

Figure 3: Left: FLADE design FPR=1.79 and Right: FLADE design FPR=2.0.

If a FLADE system is designed for low FPR such that its exhaust nozzle is unchoked, the flow variability in off-design is substantially increased. By increasing ram pressure rise from the flight the nozzle is the pushed to accept more mass flow driving the FLADE towards choke. Higher FPR points show reduced susceptibility to this effect.

3. Parametric exploration of the ACE concept

It should be emphasized that the ACE cycle studies performed in this section have not been optimized, nor have the flow variability stemming from the use of variable bypass injectors and variability geometry turbomachinery been optimized. The generated charts show the fundamental parameter dependencies of the ACE cycle.

In order to explore the performance of the ACE engine, the following flight segments of a mission have been adopted:

Table 5: Three mission phases defined for ACE "all open" (mode 1)

Case No	Altitude [m]	M_0 [-]	Net Thrust [kN]	Mission phase
01	0	0.3	105	SL runway acceleration, afterburner-on (Initial)
02	0	0.9	130	SL climb and acceleration, afterburner-on (Final)
03	91.4	0.95	35	Cruise, low altitude, afterburner-off
04	7620	0.5	15	Loiter, afterburner-off

Firstly, the mission phase results were obtained for a conventional turbofan, here, considered as a reference case for comparison with the ACE cycle. Table 7 shows the performance data for the turbofan. Notice that the leftmost column lists case numbers (No) not the mode of the engine.

Table 6: Performance data for reference turbofan engine.

Case No	ALT [m]	M_0 [-]	P_2 [kPa]	T_2 [K]	W_2 [kg/s]	P_{T3} [kPa]	T_3 [K]	P_{T4} [kPa]	T_4 [K]	P_{T5} [kPa]	T_5 [K]	ABmod [-]
1	0	0.3	105.8	293	81.4	2205	749	2114	1760	411	1138	lit
2	0	0.9	169.1	335	104.9	2818	798	2700	1843	539	1207	lit
3	91.44	0.95	177.8	339	84.2	1958	723	1872	1611	395	1060	unlit
4	7620	0.5	44.1	251	30.2	690	600	660	1387	132	886	unlit

Case No	ALT [m]	M_0 [-]	BPR1 [-]	BPR2 [-]	OPR [-]	F_N [kN]	η_{th} [-]	η_p [-]	$\eta_{Overall}$ [-]	vcore [m/s]	vflade [m/s]
1	0	0.3	0	0.52	20.9	90	0.209	0.167	0.0349	1128	0
2	0	0.9	0	0.57	16.7	107	0.244	0.402	0.0981	1239	0
3	91.44	0.95	0	0.68	11.0	35	0.403	0.616	0.2482	730	0
4	7620	0.5	0	0.57	15.7	15	0.405	0.388	0.1571	645	0

A parametric study is performed considering FPR_{FLADE} ranging from 1.3 to 2.1, and BPR1 varying from 0.1 to 2.0 for the ACE “all open” mode. For detailed studies, the FLADE operational constraints need to be managed such that the surge and choking regions are avoided adjusting the FLADE exhaust nozzle area. For some investigated cases, in particular, for low FPR_{FLADE} the variable nozzle is necessary to obtain feasible operation. However, in the present work the nozzle area will not be changed, with other words it is kept at its nominal condition. Instead, some unstable points have simply been removed from the output.

The effect of the FLADE on the ACE “all open” (mode 1) performance for the four mission phases, as defined by Table 5, will now be graphically presented. It has been considered a variation of BPR1 from 0.1 to 2.0, and FPR of the FLADE from 1.3 to 2.1. The red circle represents the turbofan engine performance data.

Figure 4 shows the thermal efficiency in function of BPR1 variation for several FPR_{FLADE}. As can be observed, due to FLADE operational constraints results were not obtained for all FPR_{FLADE} cases, particularly for values close to the lower end, due to FLADE choking. For the BPR1 parameter other limiting conditions were observed in Cases No 1, 3 and 4 due to the OPR limit (Overall Pressure Ratio), here set to 33.0. For the Case No 2 BPR1 was limited to 0.8 because of a T4 constraint achieving the max limiting value of 2,200 [K]. For Case No 3 it was observed that choking occurred for FPR_{FLADE} =1.7 in the lower BPR1 region. Higher thermal efficiencies were obtained for higher BPR1:s and lower FPR_{FLADE}. Later on, it will be shown that for lower values of FPR_{FLADE}, higher core velocities are obtained; hence, higher thermal efficiencies values are achieved. Also, it can be observed that for all investigated cases, the thermal efficiencies of the ACE “all open” (mode 1) are higher than the conventional turbofan.

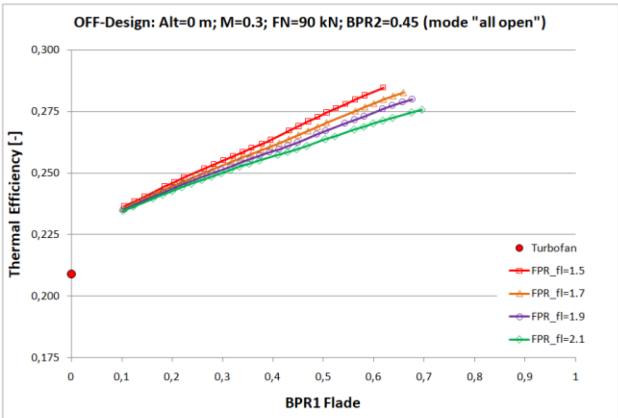

(a)

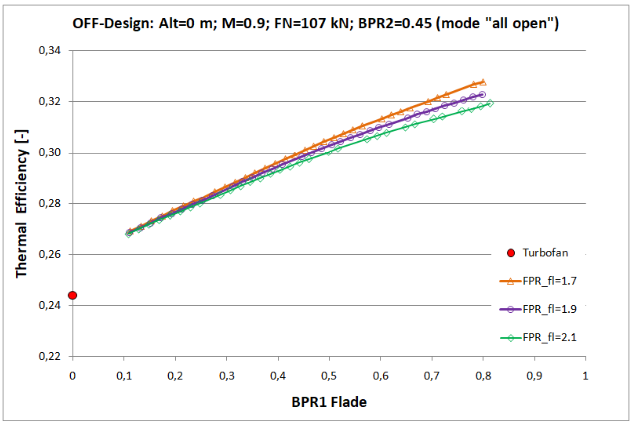

(b)

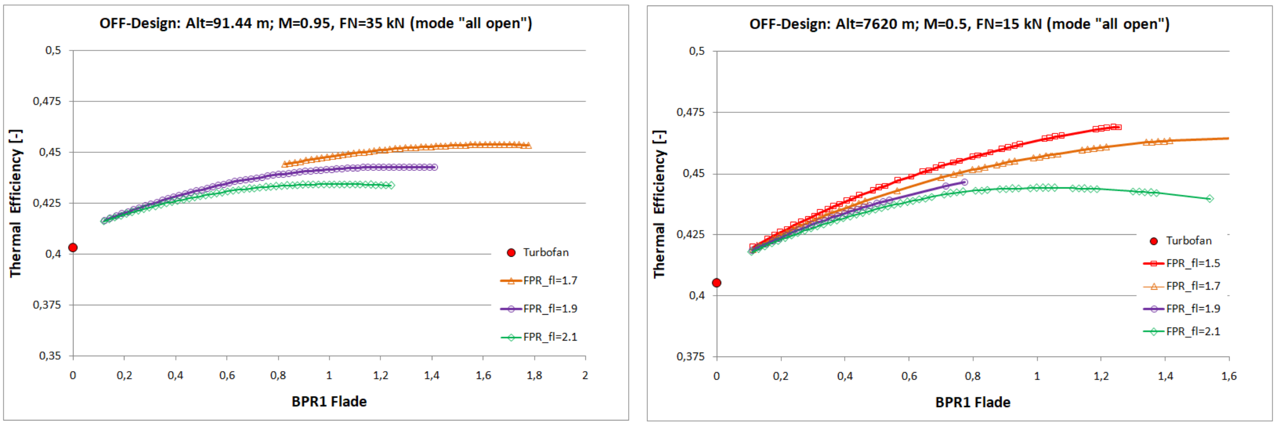

(c) (d)

Figure 4: BPR1 Effect on the ACE thermal efficiency for "all open" mode at the off-design conditions: (a) Case No 01; (b) Case No 02; (c) Case No 03; (d) Case No 04.

Propulsive efficiencies (η_p) values considering variation of FLADE BPR1 and FPR_{FLADE} were observed. Figure 5 shows a tendency of a propulsive efficiency gain as the BPR1 and FPR_{FLADE} values increase. When it is compared across the different engines, most points investigated present lower propulsive efficiencies for the ACE "all open" (mode 1) than the conventional turbofan (red circle), the exception being FPR_{FLADE}= 2.1 presenting higher propulsive efficiencies than turbofans for high values of BPR1.

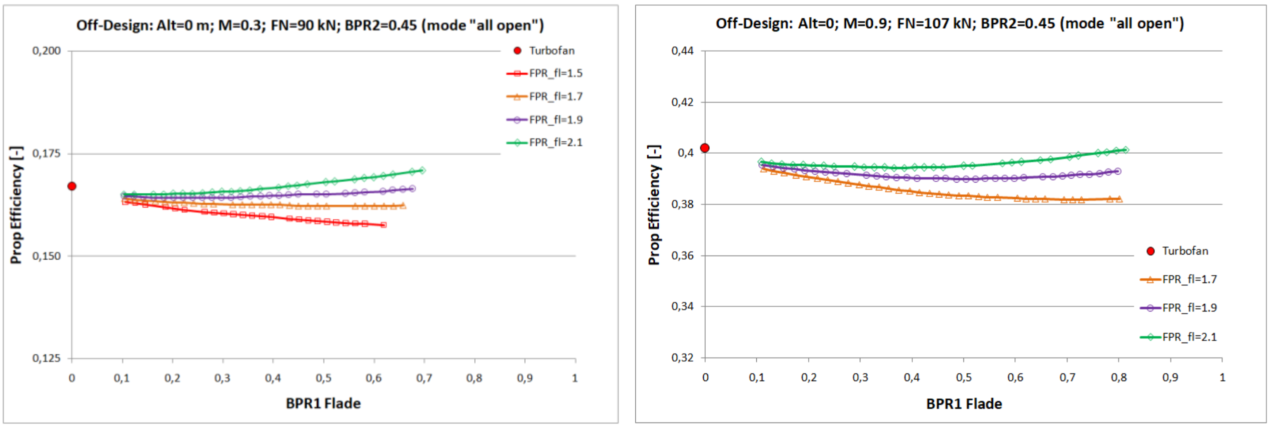

(a) (b)

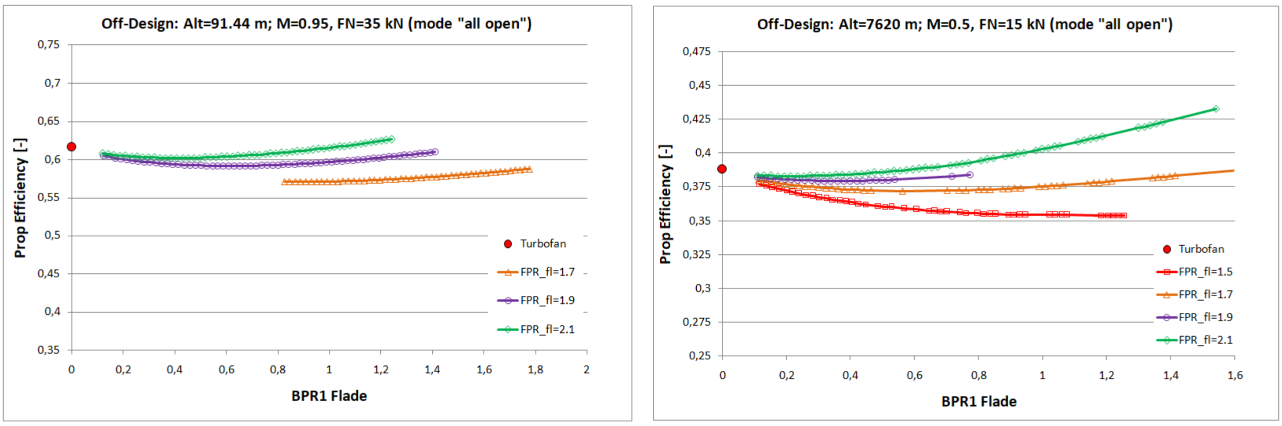

(c) (d)

Figure 5: BPR1 Effect on the ACE propulsive efficiency for "all open" mode at the off-design conditions: (a) Case No 01; (b) Case No 02; (c) Case No 03; (d) Case No 04.

Another way of analyzing the engines performance can be done by studying the overall efficiency (η_T* η_p). Figure 6 shows that as an increase in BPR1 occurs an increase in the overall efficiency is noted, and the higher values of the overall efficiency are produced for the higher FPR_{FLADE}. It can be noticed, also, in all cases investigated for the ACE "all open" (mode 1) higher overall efficiencies are obtained than for the conventional turbofan.

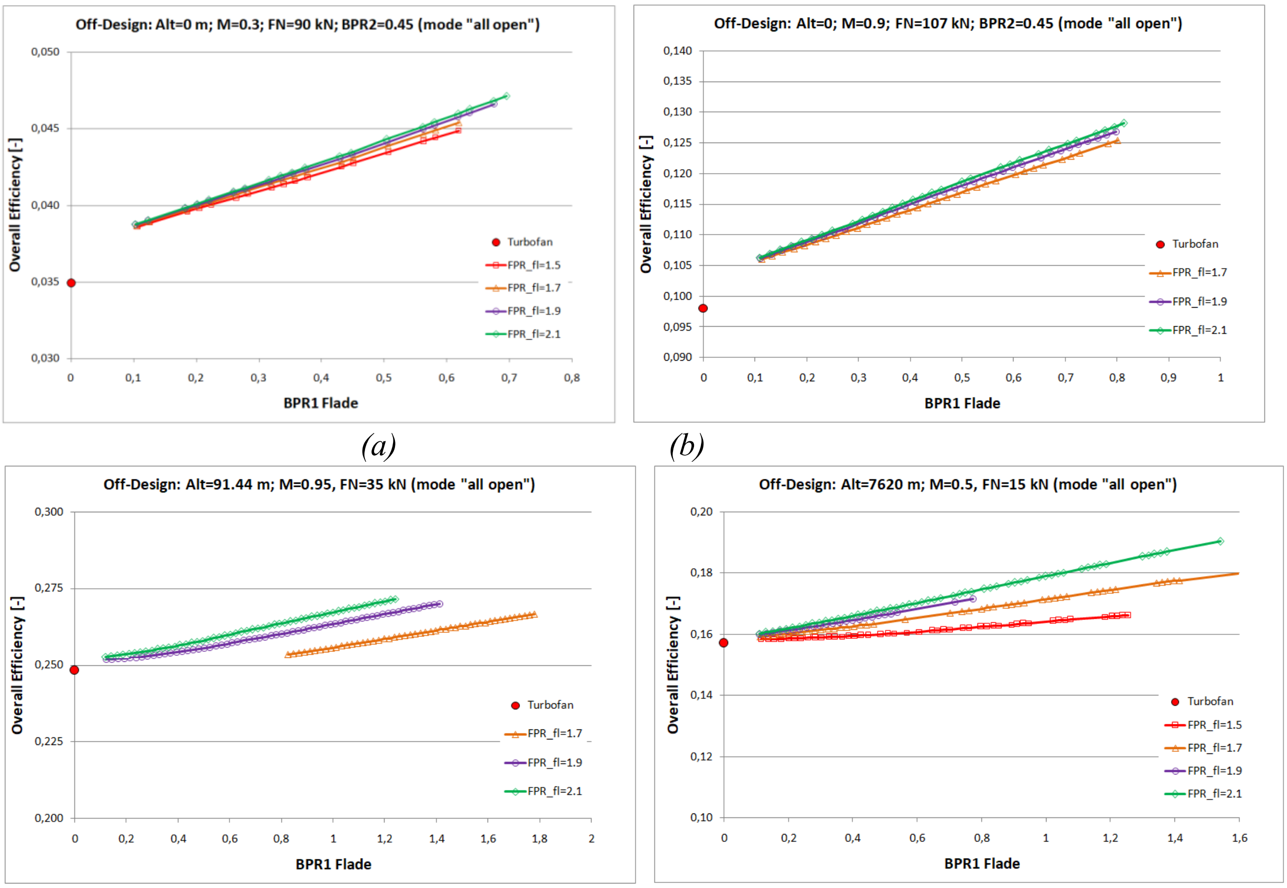

(a) (b)

(c) (d)

*Figure 6: BPR1 Effect on the ACE overall efficiency (ηT * ηp) for "all open" mode at the OFF-Design conditions: (a) Case No 01; (b) Case No 02; (c) Case No 03; (d) Case No 04.*

Figure 7 and Figure 8 present, respectively, the curves of core velocities and FLADE velocities for the ACE "all open" (mode 1). From Figure 7, it can be observed that higher core velocities occur for lower FPR_{FLADE} settings and they become even higher with the increase of BPR1. This behavior is reflected in the thermal and propulsive efficiency values presented in the previous figures.

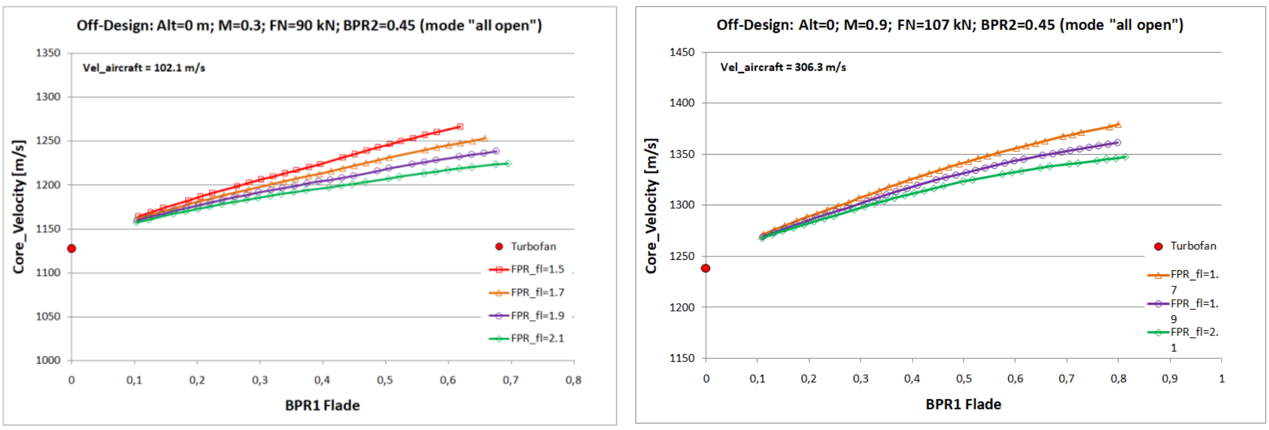

(a) (b)

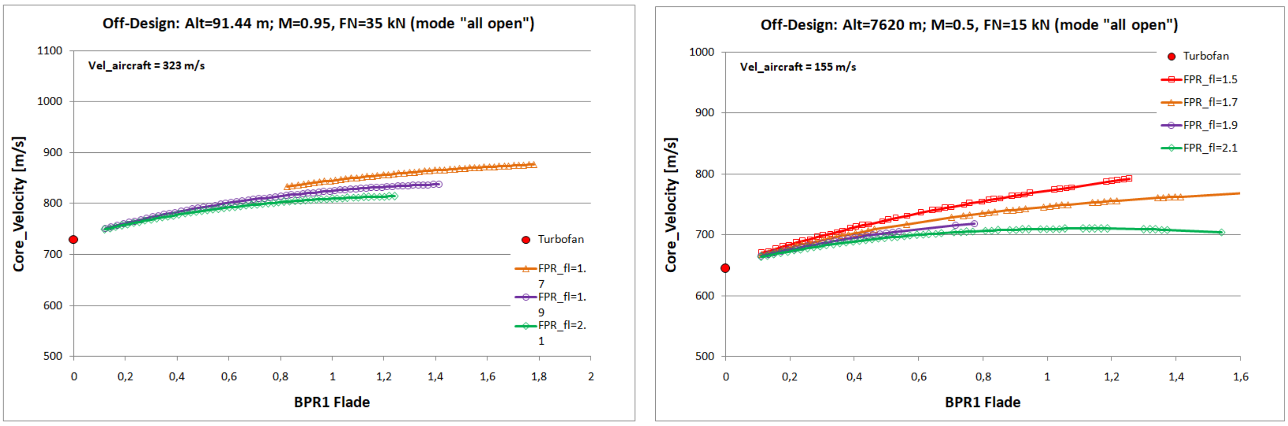

(c) *(d)*

Figure 7: BPR1 Effect on the ACE core velocity for "all open" mode at the off-design conditions: (a) Case No 01; (b) Case No 02; (c) Case No 03; (d) Case No 04.

From Figure 8 it is clear that higher FLADE exhaust velocities are obtained for higher FPR_{FLADE}. As BPR1 increases, there is evidently an increase in FLADE velocity and mass flow in the FLADE duct, hence, a decrease in the engine core flow mass (total mass flow is set fixed across all cases). The core velocities also increase, as well as the temperature T4 (burner exit temperature) with higher values of BPR1.

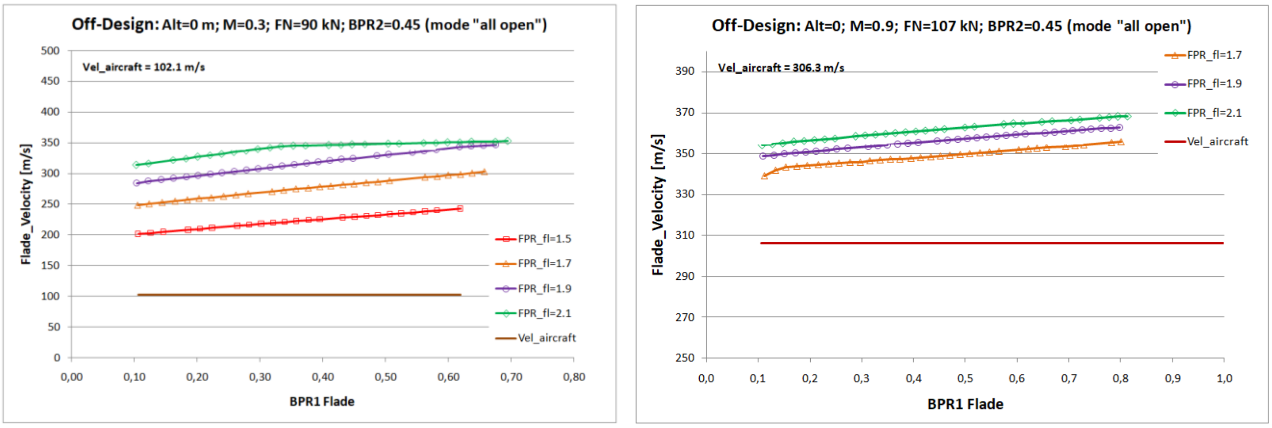

(a) *(b)*

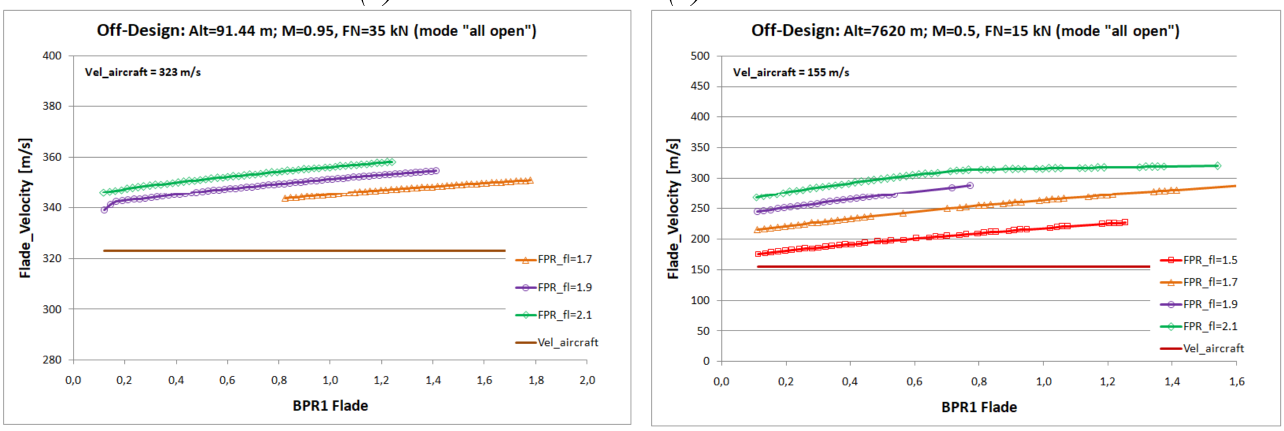

(c) *(d)*

Figure 8: BPR1 Effect on the ACE FLADE velocity for "all open" mode at the off-design conditions: (a) Case No 01; (b) Case No 02; (c) Case No 03; (d) Case No 04.

4. Range optimization of a FLADED turbofan

To conclude, we present a preliminary study on the maximization of the range of a FLADE:d turbofan by studying the specific range parameter simplified for constant level flight (L=constant), namely using $\frac{\eta_0}{\mathrm{D}}$ where the drag parameter is parameterized with the aircraft Mach number as predicted for the 9144 meter condition.

Table 7: Aircraft drag variation with Mach number for alt=9144 m.

Mach	0.45	0.50	0.55	0.60	0.65	0.70	0.75	0.80	0.85	0.90
Drag [kN]	18.5	19.2	19.9	20.7	21.6	22.7	24.2	26.1	28.6	32.3

As the Mach number is reduced the relative contribution of the FLADE stream increases allowing it to have an impact of the total performance of the engines. In addition, the BPR1 parameter now varies substantially. The optimum range is observed for a Mach number around 0.65-0.70 and a BPR close to 0.7. The 90 kg design mass flow is not allowed to vary in order to, at least to some effect, limit the influence of installation loss and engine mass variation.

The results indicate around a 4-5% range benefit in relation to the best turbofan concepts.

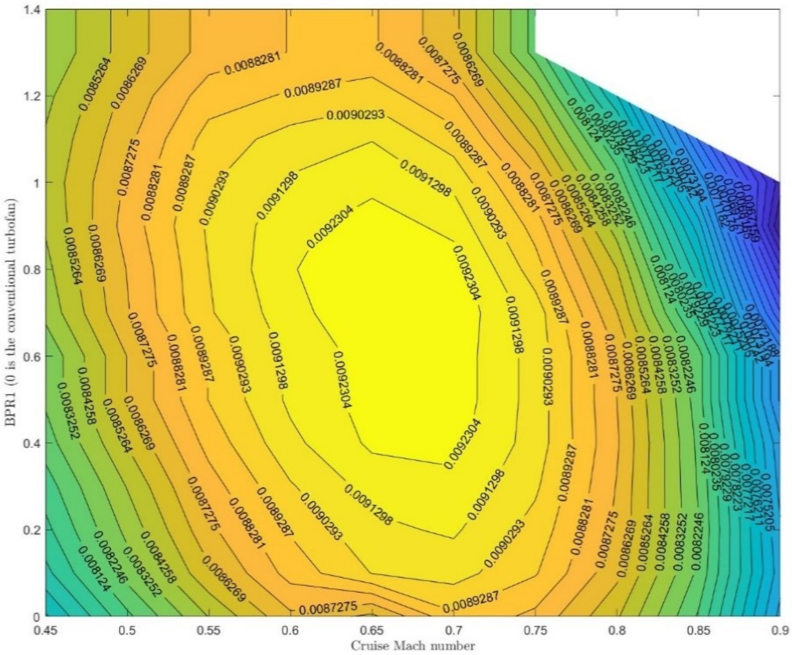

Figure 9: Variation in $\frac{\eta_0}{D}$ with Mach number and BPR1.

5. Summary and conclusion

The present study has explored some of the potential benefits of using a FLADE for a turbofan engine, primarily concentrating on its potential to extend the range of subsonic cruise. It is concluded that the high speeds used for subsonic cruise combined with the limited FLADE pressure ratio available for a single stage FLADEs, makes it difficult to reach large proportions of the total thrust contribution from the FLADE nozzle. Using lower cruise speeds in combination with higher BRP1 values may increase the range up to 5% compared to a turbofan. To fully explore the impact of the FLADE, benefits arising from flow holding and accounting for reduced installation drag needs to be considered. Such a study should be accompanied by a careful analysis of component efficiency variation and engine mass variation. Some analysis on the need for an exhaust nozzle variability in the FLADE stream is discussed, showing that there is a greater need for variability in lower speed cruise, when the FLADE design pressure ratio is lower.

References

[1] M. Corbett and J. M. Wolff, "Modeling Transient Effects of a Double Bypass Engine," in *International Energy Conversion Engineering Conference*, Nashville, TN, 2010.

[2] H. R. Patel, "Parametric Cycle Analysis of Adaptive Cycle Engine," University of Texas, Arlington, 2016.

[3] J. E. Johnson, "Variable Cycle Engine Developments at General Electric - 1955--1995," *Progress in Astronautics and Aeronautics,* vol. 165, pp. 105-158, 1996.

[4] R. V. Petrescu, The Aviation History: New Aircraft I, Lightning Source UK Ltd, 2013, p. 58.

[5] Rolls-Royce North American Technologies, "www.rolls-royce.com," [Online]. Available: https://www.rolls-royce.com/media/press-releases-archive/yr-2009/usaf-advent-research-demonstrator.aspx. [Accessed 2020].

[6] R. Brooks, "USAF Taps GE to Develop New Jet EnginesPress Release 21 October 2012,," USAF Taps GE to Develop New Jet Engines, October 2012. [Online]. [Accessed 21 December 2020].

[7] R. Grant, "Adaptive engines," *Air Force Magazine,* 2012.

[8] N. Zazulia, "Detailed Design Complete for GE´s Revolutionary Adaptive Fighter Engine," 1 March 2019. [Online]. Available: https://www.aviationtoday.com/2019/03/01/detailed-design-complete-for-ges-revolutionary-adaptive-cycle-fighter-engine/. [Accessed 22 December 2020].

[9] R. J. Simmons, "Design and Control of a Variable Geometry Turbofan with a Independently Modulated 3rd Stream," Ph.D. Dissertation,," Ohio State Univ, Columbus, Ohio, 2009.

[10] D. Rosell and T. Grönstedt, "Design Considerations of Low Bypass Ratio Mixed Flow Turbofan Engines with Large Power Extraction."," *Fluids,* vol. 7, no. 1, p. 21, 2022.

[11] J. Zheng, H. Tang and M. Y. F. J. Chen, " Equilibrium running principle analysis on an adaptive cycle engine.," *Applied Thermal Engineering,* vol. 132, pp. 393-409, 2018.

[12] J. Kurzke, "The Mission Defines the Cycle: Turbojet, Turbofan and Variable Cycle Engines for High Speed Propulsion," ADA596249, RTO-EN-AVT-185, Dachau, 2010.

[13] GE Aviation, "GE-ADAPTIVE-CYCLE-ENGINE," [Online]. Available: https://www.geaviation.com/military/engines/ge-adaptive-cycle-engine. [Accessed 23 Jan 2022].

[14] T. Grönstedt, "Development of Methods for Analysis and Optimization of Complex Jet Engine Systems. Ph.D. Thesis," Chalmers University of Technology, Göteborg, 2000.

[15] A. Rustom, A. G. Turner, A. M. Dziech, J. J. Decker and P. Szucs, "Flade fan with different inner and outer airfoil stagger angles at a shroud therebetween," EUROPEAN PATENT APPLICATION, EP1 895142A2, 2007.

[16] D. S. Lee, D. Fahey, A. Skowron, M. R. Allen, U. Burkhardt, Q. Chen, S. J. Doherty, S. Freeman, P. M. Forster, J. Fuglestvedt, A. Gettelman, R. De Leon, L. L. Lim, M. T. Lund, R. J. Millar, B. Owen, J. E. Penner, G. Pitari, M. J. Prather, R. Sausen and L. M. Wilcox, "The contribution of global aviationto anthropogenic climate forcing for 2000 to 2018," *Atmospheric Environment,* vol. 244, 2021.

[17] L. M. Dray, A. W. Schäfer and K. A. Zayat, "The Global Potential for CO2 Emissions Reduction from Jet Engine Passenger Aircraft," *Transport Research Record,* vol. 2672, no. 23, pp. 40-51, 2018.

[18] J. J. Lee, Historical and future trends in aircraft performance, cost, and emissions, Cambridge: Massachusetts Institute of Technology, 1998.

[19] J. E. Penner, D. Lister, D. Griggs, D. D. j. and M. McFarland, Aviation and the global atmosphere; a specal report of IPCC working groups I and III.", Cambridge: Cambridge University Press, 1999.

[20] N. Cumpsty, D. Mavris and M. Kirby, "Aviation and the Environement: Outlook," ICAO, 2019.

[21] E. M. Thoma and T. Z. X. Grönstedt, "Quantifying the environmental design trades for a state-of-the-art turbofan engine.," *Aerospace, ,* vol. 7, no. 10, p. 148, 2020.

[22] V. Grewe, A. Rao, T. Grönstedt, C. Xisto, F. Linke, J. Melkert, J. Middel, B. Ohlenforst, S. Blakey, S. Christie and S. Matthes, "Evaluating the climate impact of aviation emission scenarios towards the Paris agreement including COVID-19 effects," *Nature Communications,* vol. 12, no. 1, pp. 1-10, 2021.

[23] M. Lejon, T. Grönstedt, N. Glodic, P. Petrie-Repar, M. Genrup and A. Mann, "Multidisciplinary design of a three stage high speed booster.," in *In Turbo Expo: Power for Land, Sea, and Air*, Charlotte, NC, USA, 2017 .

[24] Pacelab Aircraft Preliminary Design., "PACE Aerospace Engineering & Information Technology GmbH.," Version 7.4.

[25] Airbus, "AIRCRAFT CHARACTERISTICS AIRPORT AND MAINTENANCE PLANNING - A350," Blagnac, 2019.

[26] S. Samuelsson, K. G. Kyprianidis and T. Grönstedt, "Consistent conceptual design and performance modeling of aero engines.," in *(Vol. 56673, p. V003T06A017). American Society of Mechanical Engineers.In Turbo Expo: Power for Land, Sea, and Air*, Montreal, Canada, 2015.

[27] T. Grönstedt, C. Xisto, V. Sethi, A. Rolt, N. Roas, A. Seitz, D. Misirlis, J. Whurr, N. Tantot and M. Dietz, "Conceptual design of ultra-efficient cores for mid-century aircraft turbine engines.," in *In Proceedings of the 24th ISABE*, Canberra, Australia, pp. 22-27, 2019, 2019.

[28] ICAO, "Destination green: the next chapter." Environmental Report," 2019.

[29] K. Kyprianidis and E. Dahlquist, "On the trade-off between aviation NOx and energy efficiency," *Applied Energy,* vol. 185, pp. 1506-1516., 2017.

[30] A. M. Rolt and K. Kyprianidis, "Assessment of new aero engine core concepts and technologies in the EU framework 6 NEWAC programme," in *ICAS Congress Proceedings*, 2010.

[31] K. Tacina and C. Wey, "NASA Glenn high pressure low NOx emissions research.," 2008.

[32] I. Jonsson, C. Xisto, M. Lejon, A. Dahl and T. Grönstedt, "Design and Pre-Test Evaluation of a Low-Pressure Compressor Test Facility for Cryogenic Hydrogen Fuel Integration.," in *In Turbo Expo: Power for Land, Sea, and Air*, Virtual , 2021.

[33] VINK project design, "High Speed Booster Design Data.," 20 11 2016. [Online]. Available: github.com/nikander/VINK. .

[34] A. Björkman and P. H. Mahaveer, "Aerothermal performance of fan outlet guide vanes in modern geared turbofan engines," Chalmers University of Technology, Gothenburg, 2021.

[35] A. Björkman and H. Mahaveer P., "Aerothermal performance of fan outlet guide vanes in modern geared turbofan engines," Chalmers University, Gothenburg, 2021.

[36] ICAO, "Local Air Quality Technology Standards," [Online]. Available: https://www.icao.int/environmental-protection/Pages/LAQ_TechnologyStandards.aspx. [Accessed Nov 2020].